

1 **Genome-centric analysis of short and long read metagenomes reveals
2 uncharacterized microbiome diversity in Southeast Asians**

3 Jean-Sebastien Gounot^{1*}, Chia Minghao^{1*}, Denis Bertrand^{1*}, Woei-Yuh Saw^{2,3}, Aarthi
4 Ravikrishnan¹, Adrian Low⁴, Yichen Ding⁴, Ng Hui Qi Amanda¹, Linda Wei Lin Tan⁵, Teo Yik-
5 Ying^{2,5,6#}, Henning Seedorf^{4,7#}, Niranjan Nagarajan^{1,8#}

6 ¹*Genome Institute of Singapore, Singapore 138672, Singapore*

7 ²*Life Sciences Institute, National University of Singapore, Singapore 117456, Singapore*

8 ³*Baker Heart and Diabetes Institute, 75 Commercial Rd, Melbourne 3004, Victoria, Australia*

9 ⁴*Temasek Life Sciences Laboratory, 1 Research Link, Singapore 117604, Singapore*

10 ⁵*Saw Swee Hock School of Public Health, National University of Singapore, 12 Science Drive 2,
11 Singapore 117549, Singapore*

12 ⁶*Department of Statistics and Applied Probability, National University of Singapore, Singapore
13 117546, Singapore*

14 ⁷*Department of Biological Sciences, National University of Singapore, Singapore 117558,
15 Singapore*

16 ⁸*Yong Loo Lin School of Medicine, National University of Singapore, Singapore 117596, Singapore*

17 **Joint First Authors*

18 *#Corresponding Authors*

19 *Lead Contact: nagarajann@gis.a-star.edu.sg*

20 **Abstract**

21 Despite extensive efforts to address it, the vastness of uncharacterized 'dark matter' microbial
22 genetic diversity can impact short-read sequencing based metagenomic studies. Population-
23 specific biases in genomic reference databases can further compound this problem. Leveraging
24 advances in long-read and Hi-C technologies, we deeply characterized 109 gut microbiomes from
25 three ethnicities in Singapore to comprehensively reconstruct 4,497 medium and high-quality
26 metagenome assembled genomes, 1,708 of which were missing in short-read only analysis and
27 with $>28\times$ N50 improvement. Species-level clustering identified 70 ($>10\%$ of total) novel gut
28 species out of 685, improved reference genomes for 363 species (53% of total), and discovered
29 3,413 strains that are unique to these populations. Among the top 10 most abundant gut bacteria
30 in our study, one of the species and $>80\%$ of all strains were not represented in existing
31 databases. Annotation of biosynthetic gene clusters (BGCs) uncovered more than 27,000 BGCs
32 with a large fraction (36-88%) not represented in current databases, and with several unique
33 clusters predicted to produce bacteriocins that could significantly alter microbiome community
34 structure. These results reveal the significant uncharacterized gut microbial diversity in Southeast
35 Asian populations and highlight the utility of hybrid metagenomic references for bioprospecting
36 and disease-focused studies.

37 Introduction

38 While estimates for microbial diversity on Earth vary widely, studies suggest that there are nearly
39 a million prokaryotic species of which only around 20,000 have been cultured^{1,2}. The use of
40 culture-free metagenomic techniques has therefore been key to unravel this 'dark matter' of
41 genetic diversity on Earth. Microbial communities in a wide-range of biospheres have been
42 explored, including terrestrial³, aquatic⁴ and extreme environments⁵, as well as plant, animal and
43 human-associated microbiomes⁶. Improvements in metagenomic assembly workflows^{7–11} and
44 computing resources have further enabled the assembly of these large datasets to construct
45 metagenome-assembled genomes (MAGs) that serve to augment isolate-based reference
46 genome databases^{12,13}. Despite this, existing databases only represent approximately 48,000
47 species with genome sequences, and the accuracy and completeness of short-read based MAGs
48 is frequently lower than isolate-based references².

49 Human gut metagenomes represent an area of intense scientific interest due to their
50 association with various cancers, metabolic, immunological and neurological disease
51 conditions^{14,15}. Metagenome-wide association studies frequently rely on the completeness of
52 reference genomes to correctly assign short reads to taxa, and link microbial genes and function
53 to diseases¹⁶. In particular, existing studies suggest that there might be key population-specific
54 differences in metagenomic associations with various diseases^{17–19}. The availability of a large
55 number of short-read metagenomic datasets (e.g. >20,000 for human gut in public repositories)
56 has spurred the generation of MAG reference collections based on short-read assembly^{13,20–22}.
57 While these studies have added an impressive collection of genomes to existing databases, it is
58 unclear yet if they are representative of the genetic diversity seen in gut metagenomes around
59 the world. In addition, recent advances in sequencing assays (e.g. Hi-C²³, read cloud²⁴), hybrid²⁵
60 and long-read metagenomic analysis²⁶ have sought to address the shortcomings of short-read
61 metagenomics, and opened the possibility that long-read based MAGs can provide near-
62 complete genomes rivaling isolate genomes in quality. As access to genome sequencing becomes
63 democratized and gut metagenomes are explored in understudied populations, the strategy and
64 value for establishing population-specific MAG references remains an open question.

65 Leveraging the availability of a multi-ethnic (Chinese, Malay and Indian) healthy adult
66 cohort representing major Asian populations in Singapore, a city-state with high population
67 density, we deeply characterized 109 gut metagenomes with state-of-the-art short read, long
68 read and Hi-C technologies (*Singapore Platinum Metagenomes Project – SPMP*). The resulting
69 datasets were assembled to produce high-quality references that significantly improve existing
70 databases in assembly quality (>28× N50 improvement), helped identify 70 previously
71 uncharacterized gut microbial species (>10% novel) and more than 3,400 strains in Southeast
72 Asian populations, and uncovered thousands of novel BGCs that serve as a resource for
73 bioprospecting. The ability to substantially augment existing databases through in-depth hybrid

74 metagenomic analysis highlights the value of this strategy, the importance of uncharacterized
75 microbial diversity in Asia, and serves as a template for population-specific ‘platinum’
76 metagenome references for precision medicine programs around the world.

77 **Results**

78 **Generation of a population-specific high quality gut microbial reference catalog**

79 To explore the utility of various metagenomic strategies for generating a high-quality gut
80 microbial reference database for a population, subjects from an existing multi-omics study in
81 Singapore²⁷ were recruited to provide stool samples with informed consent (n=109;
82 **Supplementary File 1, Methods**). Samples were collected using a kit designed for preserving
83 anaerobes, DNA was extracted with a protocol optimized for high molecular weight, and shotgun
84 sequencing was performed using short (Illumina, 2×151bp, average depth=9.4Gbp,
85 **Supplementary File 2**) and long read (Oxford Nanopore Technologies - ONT, median N50=8.6kbp,
86 average depth=5.8Gbp, **Supplementary File 2**) technologies, along with high-throughput
87 chromosome conformation capture (Hi-C) analysis for a subset of samples (n=24; **Supplementary**
88 **Figure 1, Supplementary File 2, Methods**). The distribution of taxa in both sequencing
89 technologies (Illumina and ONT) were confirmed to be highly concordant (median correlation
90 coefficient p=0.90), enabling joint analysis of both datasets (**Supplementary Figure 2**).

91 We next compared the commonly used short-read strategy for building MAG reference
92 collections^{13,20–22}, with a recently proposed hybrid assembly strategy²⁵, for their utility in building
93 a population-specific database (**Methods**). From a cost perspective, we noted that the hybrid
94 strategy required <\$150 in additional sequencing costs per sample (~100% increase in total cost)
95 and marginal increase in cloud computing cost per sample (**Supplementary Note 1**). This in turn
96 was observed to result in >61% increase in the number of genomes produced per sample (>15
97 additional MAGs; **Figure 1A**) with the hybrid strategy, with some samples yielding >80 genomes.
98 Overall, 4,497 MAGs were obtained with hybrid assembly for 109 samples, versus 2,789 MAGs
99 with short-reads alone (**Supplementary File 3**), with several abundant gut bacterial genera having
100 enhanced representation within hybrid assemblies (e.g. *Bifidobacterium*, *Faecalibacterium* and
101 *Blautia*; **Figure 1B**). This was observed to substantially improve read assignment to the reference
102 genome database, ensuring that much fewer genomes were not detected, and with computed
103 relative abundances being more consistent for hybrid assemblies versus short-read assemblies
104 (**Figure 1C**). Overall, hybrid assemblies consistently improved the recovery of genomes across
105 genera, with no significant bias to any specific genera, highlighting the versatility of this approach
106 (**Supplementary Figure 3**).

107 Incorporation of long-read data in hybrid assemblies enabled marked improvements in
108 assembly contiguity (>28×) as reported previously²⁵, with an average N50 of 339kbp (L50=12)
109 with hybrid assembly relative to an N50 of 12kbp with short reads alone (**Figure 1D**). This was

110 also accompanied by a notably lower level of chimerism (<10% vs >20% with short-read
111 assemblies) and similar annotated gene lengths as short-read assemblies (**Supplementary Figure**
112 **4**), suggesting that hybrid assemblies are robust to indel errors in long reads. Overall, this
113 provided higher quality genomes based on MIMAG criteria²⁸ after binning¹⁰, where many hybrid
114 MAGs had correctly reconstructed rRNA genes²⁹, and no such MAGs were obtained with short-
115 read only assembly (**Figure 1E, Methods**). To assess if the quality of MAGs could be improved
116 further, Hi-C data was used to assist in contig binning³⁰⁻³⁵. This was found to marginally increase
117 the proportion of high-quality MAGs obtained, and double the proportion of near-complete
118 genomes, with similar average assembly contiguity (**Supplementary Figure 5, Supplementary**
119 **File 3**). As the per sample cost of Hi-C analysis is currently high (>\$500), studies for generating
120 population-specific references will need to consider this cost-benefit tradeoff.

121 Hybrid assembled genomes in SPMP were assigned taxonomy based on the Genome
122 Taxonomy Database² (GTDB) and compared to existing reference genomes to assess their utility.
123 SPMP genomes were found to provide notably improved references for most GTDB species, for
124 both isolates (>6x increase in N50) as well as uncultivated organisms (>13x; **Figure 1F**). While
125 the improvement in assembly is expected for uncultivated organisms that are primarily
126 assembled using short-read metagenomics, the observed improvement for isolates (albeit
127 smaller, Wilcoxon p-value=1.25×10⁻¹¹) is noteworthy as long-read sequencing is commonly used
128 and the assembly problem is expected to be simpler. Overall, SPMP genomes provided high-
129 quality references for 110 GTDB species, 46 of which have isolates, highlighting the value of a
130 ‘platinum’ metagenomics approach for augmenting existing reference genome databases (**Figure**
131 **1G**).

132 **Asian gut metagenomes harbor substantial uncharacterized gut microbial diversity**

133 By encompassing three major Asian ethnicities (Chinese, Malay, Indian) in Singapore we
134 anticipated that the SPMP would be a useful resource to explore Southeast Asian gut microbial
135 diversity, and tested the idea of population-specific MAG reference catalogs (**Supplementary**
136 **Figure 6**). Subsampling based rarefaction analysis with SPMP MAGs showed that with as few as
137 a 100 subjects, >90% of the estimated recoverable (at the genomic level) gut microbial species
138 diversity of the Singaporean population was represented in the SPMP catalog (**Figure 2A,**
139 **Methods**). Similarly, with a reference genome collection that is 1/6th the size of a public gut
140 microbial reference database¹³ (UHGG; 18Gb vs 3Gb), SPMP can be used to identify more gut
141 bacterial reads from an independent Singaporean study (manuscript under review; 92% vs 91%),
142 and classify substantially more reads at the genome-level when database sizes are similar (81%
143 vs 67%; **Supplementary Figure 7**). These results indicate that while the urban populations in
144 Singapore have broadly similar representation of gut microbes, their genome sequences are still
145 substantially distinct to impact mapping-based gut metagenome analyses.

146 To understand microbiome variability across ethnicities and its utility to discover new
147 biological insights, we used multivariate regression analysis³⁶ to explore relationships between
148 gut metagenome composition and demographic factors (e.g. sex, age, ethnicity). Interestingly,
149 more than 60% of the taxonomic associations discovered (91 out of 133; FDR-adjusted p-
150 value<0.05) were related to ethnicity, with 23 gender-specific and 19 age-based associations
151 (**Supplementary File 4**). We then aggregated SPMP MAGs into species-level clusters (SLCs, 95%
152 identity), annotating them with publicly available reference genome collections (**Supplementary**
153 **Figure 8, Methods**) to identify 70 putative new species for which no genomes have been available
154 previously, despite large-scale MAG generation efforts^{2,13} (**Figure 2B**). Surprisingly, these putative
155 new species represent >10% of the species-level clusters obtained (n=685) and are in addition to
156 the 363 clusters that only have MAGs and no isolate genomes in existing databases (GTDB:
157 <https://gtdb.ecogenomic.org/>, based on systematic analysis of curated genomes in RefSeq:
158 <https://www.ncbi.nlm.nih.gov/refseq/> and GenBank: <https://www.ncbi.nlm.nih.gov/genbank/>).
159 More than 50% of the novel SLCs (38 out of 70) were only assembled with hybrid assembly and
160 were missing in short-read assemblies. In addition, hybrid assemblies provided a >13x median
161 N50 improvement overall, generating nearly all of the high-quality and near-complete genomes
162 for the novel SLCs (19 out of 20), highlighting the utility of this strategy for capturing microbial
163 diversity. In comparison to a recently published resource for under-represented East and South
164 Asian populations²² we found that most species were still novel (87%, 61/70) emphasizing the
165 importance of generating population-specific references.

166 Among the novel SLCs, in addition to representatives in nearly all orders commonly
167 containing gut microbes (e.g. Bacteroidales), we noted that 17 could be classified to the order
168 Coriobacteriales while an additional 7 were assigned to Christensenellales, both of which are
169 relatively understudied gut bacterial orders with high diversity in general and few isolates
170 (**Supplementary Figure 9**). Additionally, three novel SLCs with high-quality MAGs represent the
171 only available genomes for the corresponding genera (SLC637 – closest match *Phocaeicola*, <83%
172 identity; SLC487 and SLC667 – closest match *Butyricicoccus*, <81% identity), while one of the
173 novel SLCs is among the top 10 most abundant SLCs within the gut microbiomes of SPMP subjects
174 (SLC612; **Supplementary Figure 10**). We noted that SLC612 is significantly more abundant in the
175 gut microbiomes of Singaporean populations than in western subjects, potentially explaining why
176 it was not assembled in previous large-scale studies, and emphasizing the need for population-
177 specific references for even common gut bacteria (**Supplementary Figure 10**).

178 At the strain-level (99% identity), SPMP genomes were notably unique compared to
179 >200,000 genomes in the UHGG database, with 3,413 novel strains out of 3,891 (87% novel,
180 **Methods**). Among the top 20 most abundant gut bacterial species in SPMP, less than 20% of the
181 strains were represented in UHGG, with only the keystone gut commensal *Bacteroides uniformis*
182 having >40% of its strains being represented by genomes from other populations (**Figure 2C**). For

183 species that are extensively characterized due to their use as probiotics such as *Bifidobacterium*
184 *adolescentis* and *Bifidobacterium longum*, we noted that while many strain genomes have been
185 obtained from isolates (>30; **Supplementary Figure 11**), SPMP MAGs reveal an even greater
186 uncharacterized diversity in the Singaporean population (>50 novel strains; **Figure 2C**,
187 **Supplementary Figure 11**) that could be leveraged for probiotic discovery.

188 To explore the utility of the SPMP database for bioprospecting and discovering secondary
189 metabolic pathways that may be important for gut microbiome structure and function, we
190 combined comparative³⁷ and deep learning³⁸ based approaches for annotating biosynthetic gene
191 clusters with high stringency filters (BGCs, **Methods**). In total, we identified 27,084 BGCs
192 (DeepBGC: 23,175; antiSMASH: 3,909) that grouped into 16,055 gene cluster families by BiG-
193 SCAPE³⁹ (GCFs; **Figure 2D**). More than 90% of the GCFs (15,134) did not display similarity to
194 previously known BGCs in curated standard databases (antiSMASH and MIBiG) and were not
195 found in annotations within an extensive collection of gut microbial reference genomes (HRGM,
196 **Methods**), highlighting the value of using complementary algorithms for bioprospecting in new
197 populations. We estimated that >85% of SPMP GCFs were not represented in curated databases,
198 even when only a higher confidence set of predictions from antiSMASH was considered, while
199 49% of GCFs were novel even after taking into account more extensive HRGM antiSMASH
200 annotations (**Supplementary Figure 12, 13**).

201 While a significant fraction of GCFs were predicted to encode for saccharides (N=5,888,
202 37%), in line with their important functions in microbe-microbe and microbe-host interactions⁴⁰,
203 many novel GCFs appear to encode diverse bioactive compounds such as ribosomally translated
204 and post translationally modified peptides (RiPPs), polyketides and non-ribosomal peptides
205 (NRPs) (**Figure 2D**), some of which may have antimicrobial function (**Supplementary Note 2**). In
206 particular, a group of GCFs not represented in curated databases was predicted to synthesize a
207 bacteriocin in a *Blautia* species, with 3 distinct gene configurations and genes encoding enzymes
208 for peptide modification (radical SAM superfamily) and ABC transporter genes (GCF382/271/37,
209 **Figure 2E**). Analyzing the structure of the microbial community in samples with and without the
210 novel GCFs identified distinct networks, with presence of GCF382/271/37 associated with strong
211 negative correlations between the *Blautia* species and multiple *Faecalibacterium* species
212 including *Faecalibacterium prausnitzii* (**Figure 2F, Methods**). Together with the known role of
213 *Faecalibacterium* species in gut health⁴¹⁻⁴², these observations highlight the importance of
214 comprehensively identifying secondary metabolic pathways for understanding gut metagenome
215 function in human diseases.

216 **Discussion**

217 Despite the growing number of gut microbiome studies worldwide, including from remote
218 populations in the Americas⁴³ and hunter-gatherer tribes in Africa⁴⁴, the gut microbial diversity
219 of Asian populations remains understudied⁴⁵. Singapore represents a microcosm of multiple

220 major Asian ethnic populations (Chinese, Malay and Indian) living in the shared environment of
221 a modern metropolis. While there has been extensive study of gut metagenomes of ethnic
222 Chinese individuals from China, fewer studies have involved individuals from Southeast Asia and
223 India. The SPMP can thus represent an important reference for these populations, in addition to
224 Singaporean studies. More broadly, we anticipate that the microbial diversity seen in SPMP might
225 be similar to what would be observed in other major urban centers in Asia (e.g. New Delhi,
226 Jakarta, Tokyo, Hong Kong), but is likely the 'tip of the iceberg' when considering rural and
227 nomadic populations.

228 Various parameters are likely to define the appropriate strategy for a study similar to
229 SPMP in other countries, including cost, targeted quality of reference genomes, ease of
230 technology access, and availability of sufficient number of samples from a representative
231 baseline cohort in the country. While we attempted to employ multiple different technologies
232 for SPMP to get high-quality assemblies, we chose the middle-ground in terms of cost and
233 accessibility as this is an important consideration for many countries. In particular, even higher-
234 quality metagenomic assemblies are possible if HiFi reads from the Pacific Biosciences Sequel IIe
235 system are available⁴⁶. Also, the recent announcement of higher-quality reads from ONT could
236 help improve assembly further and reduce costs⁴⁷. Even as the sequencing landscape is
237 constantly changing, the results from our study suggest that high-quality population-specific
238 metagenomic references are already feasible with a modest-sized cohort and limited sequencing
239 resources.

240 The advantages of having high-quality references for metagenomics are similar to what
241 other areas of genetics and studies in model organisms have benefited from i.e. substantially
242 reduced cost and effort in future studies by: (i) allowing the use of short reads or a single
243 sequencing assay/technology, (ii) enabling increased sensitivity in identification of genomic
244 features using reference-based approaches (e.g. taxonomic classifiers for metagenomics), (iii)
245 ensuring that there are fewer 'dark matter' reads whose origin is unknown. We envisage that
246 efforts such as SPMP will benefit the scientific community by spurring greater adoption of
247 reference-based analyses in metagenome-wide association studies^{48,49}. Additionally, as we noted
248 in **Figures 1F and 1G**, the quality of genomes that can be obtained using metagenomics is now
249 comparable or better than what can be obtained from the sequencing of microbial isolates,
250 especially with short reads. This can galvanize efforts to genetically map microbial ecosystems in
251 diverse biospheres, further contributing to the references available to study human
252 microbiomes, and understanding of strain sharing between humans and the environment. As
253 sequencing costs, ease of use and accessibility of new technologies, and metagenomic assembly
254 algorithms improve, we can expect that a majority of the high-quality microbial references that
255 will be used in the future would be obtained through metagenomics, thus helping to bridge the

256 knowledge gap for the hundreds of thousands of microbial species that are estimated to be there
257 on Earth.

258 The detection of 70 putative novel species in SPMP is perhaps not surprising given the unexplored
259 microbial diversity and the limitations of current genetic databases. However, it is noteworthy
260 that this is still a substantial fraction of the species detected in this study (>10%, **Figure 2B**), and
261 while some of these species are not frequently detected across individuals, one of them was in
262 the top 10 most abundant gut bacterial species, while others may still play a significant role in
263 the biology of some individuals by being sporadically abundant (e.g. SLC665 which is among the
264 top 20 most abundant species in 5% of subjects). Not surprisingly, at the strain-level an even
265 larger fraction of the observed genetic diversity was novel, but what was notable was that this
266 was true even for the more abundant and well-studied species in the gut microbiome (e.g.
267 *Bacteroides uniformis* and *Bifidobacterium adolescentis*, **Figure 2C**). These observations highlight
268 the overall value of such studies for discovering probiotic strains that could be leveraged for
269 population health, with modest investments in metagenomic analysis cost (<\$40,000), making it
270 feasible for national microbiome projects around the world.

271 Finally, the identification of >23,000 BGCs in the SPMP database that were not represented in
272 existing annotated databases (88% of total, **Figure 2D**) highlights that we are only scratching the
273 surface in terms of harnessing microbial pathways and functions for synthetic biology and
274 biotechnology applications. This was made possible by the high-contiguity of our hybrid
275 assemblies (>28× N50 relative to short-read assemblies), and the characterization of distinct,
276 underrepresented South-East Asian populations in SPMP harboring substantial novelty relative
277 to curated BGC databases (>85%) and annotated reference genomes (49%, **Supplementary**
278 **Figure 12, 13**). The gut microbiome by virtue of being a dynamic, host-associated community with
279 high diversity of microbes is a rich hunting ground for host-modulating, macro-nutrient
280 catabolizing and micro-nutrient synthesizing functions^{50,51}. In addition, homeostasis in the gut
281 microbiome may be maintained by key members of the community through the selective
282 expression of antimicrobial peptides⁵² (AMPs), and correspondingly we identified hundreds of
283 novel BGCs encoding putative bacteriocins, sactipeptides, lanthipeptides and lassopeptides that
284 can now be further characterized (**Supplementary Note 2**). Notably, we found evidence that the
285 presence of a BGC in a common *Blautia* species is associated with significant changes in overall
286 gut microbiome community structure for SPMP subjects (**Figure 2F**). Together these results
287 highlight the potential for novel AMPs discovered in SPMP to provide genetic templates for
288 further optimization, and subsequent use to modulate the gut microbiome, or as new
289 antimicrobials to target multi-drug resistant pathogens.

290 **Figure Legends**

291 **Figure 1. Assembly strategy for high-quality microbiome references.** (A) Boxplots showing the
292 number of MAGs obtained across metagenomic datasets using short-read and hybrid assemblies
293 (n=109). (B) Stacked barchart showing genus-specific breakdown of the number of MAGs
294 obtained using short-read and hybrid assemblies (left) and boxplots for corresponding relative
295 abundances of the genera (right). (C) Scatter-plot showing the relative abundance of
296 *Bifidobacterium* genomes estimated using short-read or hybrid assemblies for a sample (y-axis)
297 versus corresponding relative abundances obtained using the default Kraken2 database (x-axis).
298 (D) Violin plots showing the distribution of a contiguity metric (N50 – largest contig size where
299 >50% of the genome is in larger contigs) for short-read and hybrid assembly based MAGs. (E)
300 Stacked barcharts showing the relative proportion of MAGs satisfying different MIMAG quality
301 standards with short-read and hybrid assemblies of SPMP datasets. (F) Violin plots showing the
302 relative improvement in contiguity (N50) obtained using hybrid assembly MAGs from SPMP
303 relative to matched genomes in the GTDB database. (G) Barcharts showing the number of GTDB
304 reference genomes which were improved from medium to high MIMAG quality using SPMP
305 MAGs. Center lines in the boxplots represent median values, box limits represent upper and
306 lower quartile values, whiskers represent 1.5 times the interquartile range above the upper
307 quartile and below the lower quartile, and all data points are represented as dots in the figures.

308 **Figure 2. Characterization of novel species, strains and gene families in SPMP genomes.** (A)
309 Collection curve analysis showing that the SPMP database covers a substantial fraction of the
310 species level diversity in its MAGs. (B) Pie-chart showing the breakdown of species-level clusters
311 in SPMP that have an *isolate* genome, only have MAGs (*uncultivated*) and are *novel* compared to
312 genomes in public databases (UHGG, GTDB, SGB). (C) Stacked barcharts showing the number of
313 SPMP strains that have an *isolate* genome, only have MAGs (*uncultivated*) and are *novel*
314 compared to all UHGG genomes (>200,000, <99% ANI). The species shown are the top 20 in terms
315 of median relative abundance in SPMP (most abundant on the left). (D) Stacked barcharts
316 showing the number of BGCs (top) and GCFs (bottom) in different product classes that are
317 present or absent in existing annotations comprising of the antiSMASH and MiBIG databases as
318 well as antiSMASH annotations from HRGM. Inset piecharts show the overall breakdown. (E)
319 Synteny plots showing the conservation of gene order and orientation (colored arrows,
320 relatedness shown by vertical lines) for a novel GCF (GCF382) and related families. (F) Network
321 diagrams depicting correlations between gut microbial species (nodes – species, edges –
322 significant correlations) and overall microbiome structure in SPMP metagenomes when stratified
323 based on presence or absence of GCF 382/271/37 (or missing the corresponding transporter
324 gene) in a *Blautia* species (enlarged teal node, solid edges to correlated species, dashed edges
325 between other nodes).

326 **Methods**

327 **Subject recruitment**

328 Subjects for this study were recruited based on recall from a community-based multi-ethnic
329 prospective cohort²⁷ that is part of the Singapore Population Health Studies project (SPHS -
330 formerly Singapore Consortium of Cohort Studies). Subjects in SPHS were recruited to participate
331 in the National Health Survey, where subjects were selected at random using age- and gender-
332 stratified sampling to obtain a representative sample set of residents in the country. At the point
333 of recruitment in 2008, subjects did not have any pre-existing major health conditions
334 (cardiovascular disease, mental illness, diabetes, stroke, renal failure, hypertension and cancer)
335 based on self-reporting²⁷. The ethnicity of each subject was confirmed verbally so that all four
336 grandparents of the subject belonged to the same ethnic group. Informed consent was obtained
337 from all participants and the associated protocols for this study were approved by the National
338 University of Singapore Institutional Review Board (IRB reference number H-17-026).

339 **Sample collection**

340 Fecal samples were collected from healthy subjects using the BioCollector™ kit (The
341 BioCollective, Colorado, USA). Samples were kept at -20°C until they were brought into an
342 anaerobic chamber (atmosphere of N₂ (75%), CO₂ (20%) and H₂ (5%)). Fecal samples were
343 homogenized and subsamples transferred into sterile 2 mL centrifuge tubes.

344 **DNA extraction**

345 Genomic DNA was extracted from fecal material (0.25 g wet weight) using the QIAamp Power
346 Fecal Pro DNA kit (QIAGEN GmbH, Cat. No. 51804) and was quantified using Qubit dsDNA BR
347 Assay Kit (Thermo Fisher Scientific, Cat. No. Q32853). Integrity of the extracted DNA was verified
348 using 0.5% agarose gel electrophoresis.

349 **Illumina library preparation and sequencing**

350 Metagenomic libraries were prepared with a standard DNA input of 50ng across all samples,
351 using NEBNext® Ultra™ II FS DNA Library Prep Kit for Illumina (New England Biolabs, Cat. No.
352 E7805), according to the manufacturer's instructions. The reaction volumes were, however,
353 scaled to a quarter of the recommended volumes for cost effectiveness. Barcoding and
354 enrichment of libraries was carried out using NEBNext® Multiplex Oligos for Illumina® (96 Unique
355 Dual Index Primer Pairs; New England Biolabs, Cat. No. E6440). Paired-end sequencing (2×151bp
356 reads) was carried out on the Illumina HiSeq4K platform.

357 **ONT library preparation and sequencing**

358 Purity and integrity of DNA was assessed and ensured to fall within recommended ranges before
359 library preparation. To preserve the integrity of DNA, the shearing step was omitted and DNA

360 was used directly for DNA repair and end-prep. Single-plex libraries were prepared using 1D
361 sequencing kit (Oxford Nanopore Technologies, SQK-LSK108 or SQK-LSK109) according to the “1D
362 Genomic DNA by ligation” protocol. For samples that were multiplexed (12-plex), the native
363 barcoding kit (Oxford Nanopore Technologies, EXP-NBD103 or EXP-NBD104 and EXP-NBD114)
364 was used and libraries were prepared according to the “Native barcoding genomic DNA”
365 protocol. Both native barcode ligation and adapter ligation steps were extended to 30 min
366 instead of 10 min. Single-plex samples were sequenced on either the MinION or GridION machine
367 with either FLO-MIN106D or MIN106 revD flowcells. Multiplex samples were sequenced on the
368 PromethION machine with FLO-PRO002 flowcells. Raw reads were basecalled with the latest
369 version of the basecaller available at the point of sequencing (Guppy v3.0.4 to v3.2.6). Basecalled
370 nanopore reads were demultiplexed and filtered for adapters with qcat (v1.1.0
371 <https://github.com/nanoporetech/qcat>).

372 **Hi-C library preparation and sequencing**

373 Hi-C libraries were generated using Phase Genomics ProxiMeta kit (version 3.0), based on the
374 standard protocol. Briefly, 500 mg fecal material was crosslinked for 15 minutes at room
375 temperature with end-over-end mixing in 1 mL of ProxiMeta crosslinking solution. Once
376 crosslinking reaction was terminated, quenched fecal material was rinsed. Sample was
377 resuspended and a low-speed spin was used to clear large debris. Chromatin was bound to SPRI
378 beads and incubated for 1 hour with 150 µL of ProxiMeta fragmentation buffer and 11 µL of
379 ProxiMeta fragmentation enzyme. Once washed, beads were resuspended with 100 µL of
380 ProxiMeta Ligation Buffer supplemented with 5 µL of Proximity ligation enzyme and incubated
381 for 4 hours. After reversing crosslinks, the free DNA was purified with SPRI and Hi-C junctions
382 were bound to streptavidin beads and washed to remove unbound DNA. Washed beads were
383 used to prepare paired-end deep sequencing libraries using ProxiMeta Library preparation
384 reagents. Paired-end sequencing (2×151bp reads) was carried out on the Illumina HiSeq4K
385 platform.

386 **Sequence quality assessment**

387 Illumina and ONT read statistics were generated with Fastq-Scan (v0.4.1,
388 <https://github.com/rpetit3/fastq-scan>) and NanoStat⁵³ (v1.4.0), respectively. To assess
389 taxonomic concordance, Illumina and ONT reads were classified with Kraken2⁵⁴ (v2.1.1, UHGG
390 database¹³) and relative abundances were estimated with Bracken⁵⁵ (v2.6.1) at the species level
391 (option -l R7) to compute Pearson correlation coefficients per sample.

392 **Metagenomic assembly and binning**

393 Illumina reads were assembled using MEGAHIT⁸ (v1.04, default parameters) and hybrid
394 metagenomic assemblies were generated with Illumina and ONT data using OPERA-MS²⁵ (v0.9.0,
395 --polish). Contigs were binned with MetaBAT2¹⁰ (v2.12.1, default parameters). Hi-C binning was

396 provided by Phase Genomics using its internal pipeline with MetaBAT results for hybrid
397 assemblies as a starting point. Assembly bins were evaluated based on MIMAG standards²⁸, with
398 contamination, completeness and N50 values determined with CheckM⁵⁶ (v1.04), and non-
399 coding RNA annotations from barrnap (<https://github.com/tseemann/barrnap>) (v0.9) and
400 tRNAscan-SE⁵⁷ (v2.0.5, default parameters). Assembly bins with contamination <10% and
401 completeness >50% were designated as *medium quality* MAGs, those with contamination <5%
402 and completeness >90% as *near complete* MAGs, and additionally near complete MAGs with
403 complete 5S, 16S and 23S rRNA genes and at least 18 unique tRNA genes were classified as *high*
404 *quality* MAGs. All other bins were classified as *low quality* and were removed from further
405 analyses. In total, 4,497 medium quality, near complete and high quality MAGs were designated
406 as being part of the SPMP database. Hybrid and short-reads assembly based MAGs were further
407 assessed for chimerism with GUNC⁵⁸ (v1.0.4, detailed output). Coding sequence lengths obtained
408 from Prodigal⁵⁹ (v2.6.3) calls were compared between the two datasets to assess the potential
409 impact of long read indel errors on gene annotation. Concordant with prior work showing that
410 hybrid metagenomic assemblies can have high base-pair accuracy²⁵, we also noted that SPMP
411 MAGs independently assembled from distinct individual gut metagenomes could exhibit high
412 average nucleotide identity (>99.99%, consistent with Q40 quality).

413 **Annotation of MAGs with the Genome Taxonomy Database**

414 The SPMP database was compared to the GTDB database² (release 95) using GTDBTk's⁶⁰ (v1.4.1)
415 ani_rep command with default arguments, which leverages MASH⁶¹ (v2.3) to provide pairwise
416 genome-wide similarity values between all query MAGs and GTDB sequences. Only pairs with
417 MASH distance ≤ 0.05 were retained and used to define the best match for each SPMP MAG based
418 on minimum MASH distance. GTDB matches were classified based on their metadata as being
419 *uncultivated* ("derived from environmental sample" or "derived from metagenome") or based
420 on *isolate* strains. Both N50 values and MIMAG classifications were extracted from GTDB
421 metadata. MAGs were placed into a phylogenetic tree using GTDB_TK (v1.4.1) with classify_wf
422 (default options), based on pplacer_taxonomy values. To assess novelty in light of the latest
423 human gut metagenome database, we further compared our MAGs to the 5,414 representative
424 genomes from the Human Reference Gut Microbiome catalog (HRGM)²² with a similar MASH
425 analysis (**Supplementary File 5**).

426 **Species and strain-level clustering**

427 MAGs were clustered at the species (95%) and strain-level (99%) based on average nucleotide
428 identity estimates (ANI; using MASH with sketch size of 10k and k-mer size of 21bp) with
429 agglomerative clustering (sklearn v0.23.2, AgglomerativeClustering function, options:
430 linkage="single", n_clusters=None, compute_full_tree=True, affinity="precomputed"). For each
431 cluster, *representative* MAGs were defined using the highest eigen centrality value based on a
432 weighted network graph produced by networkx (v2.5; eigenvector_centrality function). Strain-

433 level clustering was done jointly with all species-level matches from the UHGG database (v1.0,
434 ANI threshold of 95%). Phylogenetic analysis at the strain-level was conducted using the
435 biopython Phylo package⁶², based on pairwise distances generated with FastANI⁶³ (v1.32).
436 Phylogenetic trees were visualized using FigTree (tree.bio.ed.ac.uk/software/figtree).

437 **Species assignment**

438 Species-level clusters (SLCs) were assigned putative species name and types based on
439 comparisons with multiple databases, including GTDB, Pasolli et al⁶⁴ (SGB) and Almeida et al¹³
440 (UHGG). SLCs types were defined as, (i) isolate: if GTDB match to an isolate was found (mash
441 distance ≤ 0.05), (ii) uncultivated: if a match to any database was found, but no isolates, (iii) novel:
442 if no matches were found. SLCs were assigned putative species names based on a majority rule
443 for MAGs in the cluster, with preference for GTDB ids (**Supplementary Figure 8**).

444 **Species abundance and rarefaction analysis**

445 Representative MAGs for SLCs were used to create a custom Kraken⁶⁵ (v2.1.1) database
446 (<https://github.com/DerrickWood/kraken2/wiki/Manual#custom-databases>) and relative
447 abundances for SLCs were estimated for each sample using Bracken⁵⁵ (v2.6.0, default
448 parameters). Rarefaction analysis for estimating overall species diversity was done using the R
449 package iNext⁶⁶ (v2.1.7, q=0, datatype="incidence_raw" and endpoint=300), based on converting
450 SLC relative abundance values from Bracken into presence-absence values at a threshold of
451 0.05%.

452 **Multivariate regression analysis**

453 Genus-level abundances for each sample were provided as input for R package MaasLin2³⁶
454 (v1.4.0) along with sample metadata (age, sex and ethnicity), and significant associations were
455 determined by combining 3 MaasLin2 runs with a compound Poisson linear model.

456 **Biosynthetic gene cluster identification and clustering**

457 Biosynthetic gene clusters (BGCs) in the SPMP database were identified using antiSMASH⁶⁷
458 (v5.1.2, --genefinding-tool prodigal-m --cb-general --cb-knownclusters --cb-subclusters --asf --
459 pfam2go --smcog-trees) and DeepBGC³⁸ (v0.1.18, prodigal-meta-mode). BGCs with only one
460 identified gene and with length $< 2\text{ kbp}$ were removed for both sets of results. For antiSMASH this
461 provided a set of 3,909 BGCs. DeepBGC results which overlapped with antiSMASH were removed
462 if the genomic coordinates of both BGCs overlapped by $\geq 30\%$ in either direction. DeepBGC
463 candidates were further filtered for i) being categorized with a known product class and ii)
464 containing at least one known biosynthetic pfam or TIGRFAM protein domain as defined by
465 Cimermancic et al⁶⁸, providing an additional set of 23,175 BGCs.

466 All 27,084 BGCs (3,909 from antiSMASH + 23,175 from DeepBGC) were first categorized into
467 different product classes: ribosomally synthesized and post-translationally modified peptides

468 (RiPPs), nonribosomal peptide synthetases (NRPs), polyketide synthases (PKS), saccharides and
469 others based on the labels reported by each algorithm. We further unified the antiSMASH and
470 DeepBGC product class labels to integrate both datasets (**Supplementary Table 1**). A fraction of
471 mined BGCs were labeled as “hybrids” because antiSMASH or DeepBGC associated them with
472 two different product classes e.g. “bacteriocin;T1PKS”. The BGCs in each product class were
473 grouped into gene cluster families (GCFs) by sequence similarity using BiG-SCAPE³⁹ (v1.01, --
474 include_singletons --mix --no_classify --cutoffs 0.3). A total of 16,055 GCFs were defined by this
475 approach and for each GCF we took the smallest BGC member as a representative of the family.
476 Gene cluster diagrams of BGCs were created using Clinker⁶⁹.

477 BGCs in SPMP were classified as *novel* via a two-step approach. Firstly, BGC sequences were
478 required to have <80% similarity to any existing sequence in the antiSMASH and MIBiG 2.0⁷⁰
479 databases using the clusterblast results from antiSMASH. Secondly, BGC annotations were
480 compared to antiSMASH annotations from a comprehensive gut microbial genome collection
481 (HRGM) using the standalone clusterblast software⁷¹ (v 1.1.0), to identify SPMP matches based
482 on a 80% similarity threshold, similar to the approach described in Gallagher et al⁷².

483 **Characterization of antimicrobial peptides and impact on microbiome structure**

484 Antimicrobial activities of putative peptides encoded by novel RiPP BGCs in SPMP were predicted
485 using an ensemble voting approach with four different antimicrobial peptide (AMP) prediction
486 models: AMPscanner⁷³ (v2, convolutional neural network), AmpGram⁷⁴ (random forest model),
487 AMPDiscover⁷⁵ (based on quantitative sequence activity models) and ABPDiscover
488 (<https://biocom-ampdiscover.cicese.mx/>). Peptides predicted by antiSMASH in these RiPP BGCs
489 were translated and all amino acid sequences with a length greater than 10 but lesser than 200
490 were used as inputs into these four models. Peptides were classified as AMPs if they received
491 votes from both AMPscanner and AmpGram, and at least one vote from either AMPDiscover or
492 ABPDiscover, and corresponding RiPP BGCs contained a transporter protein. The performance of
493 this ensemble approach was evaluated using 78 known AMP sequences and 78 scrambled non-
494 AMP sequences taken from the AmpGram benchmark dataset⁷⁴. For our evaluation dataset, we
495 identified and removed all sequences that were found in the training sets of AMPscanner,
496 AmpGram, AMPDiscover and ABPDiscover using seqkit⁷⁶ (v0.11.0) and samtools faidx (v1.9). The
497 percentage hydrophobicity and overall charge of selected peptide sequences was determined
498 using the antimicrobial peptide calculator in the antimicrobial peptide database 3 (APD3;
499 <https://aps.unmc.edu/prediction>).

500 To associate BGC presence/absence patterns with microbial community structure, correlation
501 analysis (Fastspar⁷⁷ v1.0.0, parameters: --iterations 100 --exclude_iterations 20, p-values from
502 1000 bootstrap replicates and permutation testing) was done based on SLC abundance profiles
503 across samples (species with medium abundance ≤0.1% filtered out). Correlations in the network
504 were kept if they had an associated p-value <0.05.

505 **Data and source code availability**

506 Shotgun metagenomic sequencing data (Illumina and ONT) are available from the European
507 Nucleotide Archive (ENA – <https://www.ebi.ac.uk/ena/browser/home>) under project accession
508 number PRJEB49168. Source code for scripts used to analyze the data are available in a GitHub
509 project at <https://github.com/CSB5/SPMP>.

510 References

- 511 1. Curtis, T. P., Sloan, W. T. & Scannell, J. W. Estimating prokaryotic diversity and its limits.
512 *Proc. Natl. Acad. Sci.* **99**, 10494–10499 (2002).
- 513 2. Parks, D. H. *et al.* GTDB: an ongoing census of bacterial and archaeal diversity through a
514 phylogenetically consistent, rank normalized and complete genome-based taxonomy.
515 *Nucleic Acids Res.* **1**, 13–14 (2021).
- 516 3. Nayfach, S. *et al.* A genomic catalog of Earth's microbiomes. *Nat. Biotechnol.* **39**, 499–509
517 (2021).
- 518 4. Tully, B. J., Graham, E. D. & Heidelberg, J. F. The reconstruction of 2,631 draft
519 metagenome-assembled genomes from the global oceans. *Sci. Data* **5**, 1–8 (2018).
- 520 5. Tyson, G. W. *et al.* Community structure and metabolism through reconstruction of
521 microbial genomes from the environment. *Nature* **428**, 37–43 (2004).
- 522 6. Tierney, B. T. *et al.* The landscape of genetic content in the gut and oral human
523 microbiome. *Cell Host Microbe* **26**, 283–295.e8 (2019).
- 524 7. Li, D., Liu, C. M., Luo, R., Sadakane, K. & Lam, T. W. MEGAHIT: An ultra-fast single-node
525 solution for large and complex metagenomics assembly via succinct de Bruijn graph.
526 *Bioinformatics* **31**, 1674–1676 (2015).
- 527 8. Li, D. *et al.* MEGAHIT v1.0: A fast and scalable metagenome assembler driven by
528 advanced methodologies and community practices. *Methods* **102**, 3–11 (2016).
- 529 9. Kolmogorov, M., Rayko, M., Yuan, J., Polevikov, E. & Pevzner, P. MetaFlye: Scalable long-
530 read metagenome assembly using repeat graphs. *bioRxiv* 637637 (2019).
531 doi:10.1101/637637
- 532 10. Kang, D. D. *et al.* MetaBAT 2: An adaptive binning algorithm for robust and efficient
533 genome reconstruction from metagenome assemblies. *PeerJ* **2019**, (2019).
- 534 11. Wu, Y. W., Simmons, B. A. & Singer, S. W. MaxBin 2.0: An automated binning algorithm
535 to recover genomes from multiple metagenomic datasets. *Bioinformatics* **32**, 605–607
536 (2016).
- 537 12. Parks, D. H. *et al.* A standardized bacterial taxonomy based on genome phylogeny
538 substantially revises the tree of life. *Nat. Biotechnol.* **36**, 996 (2018).
- 539 13. Almeida, A. *et al.* A unified catalog of 204,938 reference genomes from the human gut
540 microbiome. *Nat. Biotechnol.* **39**, 105–114 (2021).
- 541 14. Kishikawa, T. *et al.* Metagenome-wide association study of gut microbiome revealed
542 novel aetiology of rheumatoid arthritis in the Japanese population. *Ann. Rheum. Dis.* **79**,
543 103–111 (2020).
- 544 15. Zhu, F. *et al.* Metagenome-wide association of gut microbiome features for
545 schizophrenia. *Nat. Commun.* **11**, (2020).
- 546 16. Wang, J. & Jia, H. Metagenome-wide association studies: Fine-mining the microbiome.
547 *Nature Reviews Microbiology* **14**, 508–522 (2016).

548 17. Zhernakova, A. *et al.* Population-based metagenomics analysis reveals markers for gut
549 microbiome composition and diversity. *Science* **352**, 565–569 (2016).

550 18. Falony, G. *et al.* Population-level analysis of gut microbiome variation. *Science* **352**, 560–
551 564 (2016).

552 19. Breuninger, T. A. *et al.* Associations between habitual diet, metabolic disease, and the
553 gut microbiota using latent Dirichlet allocation. *Microbiome* **9**, 1–18 (2021).

554 20. Zou, Y. *et al.* 1,520 reference genomes from cultivated human gut bacteria enable
555 functional microbiome analyses. *Nat. Biotechnol.* **37**, 179–185 (2019).

556 21. Forster, S. C. *et al.* A human gut bacterial genome and culture collection for improved
557 metagenomic analyses. *Nat. Biotechnol.* **37**, 186–192 (2019).

558 22. Kim, C. Y. *et al.* Human reference gut microbiome catalog including newly assembled
559 genomes from under-represented Asian metagenomes. *Genome Med.* **13**, (2021).

560 23. Burton, J. N., Liachko, I., Dunham, M. J. & Shendure, J. Species-level deconvolution of
561 metagenome assemblies with Hi-C-based contact probability maps. *G3 Genes, Genomes,*
562 *Genet.* **4**, 1339–1346 (2014).

563 24. Bishara, A. *et al.* High-quality genome sequences of uncultured microbes by assembly of
564 read clouds. *Nat. Biotechnol.* **36**, 1067–1080 (2018).

565 25. Bertrand, D. *et al.* Hybrid metagenomic assembly enables high-resolution analysis of
566 resistance determinants and mobile elements in human microbiomes. *Nat. Biotechnol.*
567 **37**, 937–944 (2019).

568 26. Kolmogorov, M., Yuan, J., Lin, Y. & Pevzner, P. A. Assembly of long, error-prone reads
569 using repeat graphs. *Nat. Biotechnol.* **37**, 540–546 (2019).

570 27. Saw, W. Y. *et al.* Establishing multiple omics baselines for three Southeast Asian
571 populations in the Singapore Integrative Omics Study. *Nat. Commun.* **8**, (2017).

572 28. Bowers, R. M. *et al.* Minimum information about a single amplified genome (MISAG) and
573 a metagenome-assembled genome (MIMAG) of bacteria and archaea. *Nature*
574 *Biotechnology* **35**, 725–731 (2017).

575 29. Parks, D. H. *et al.* Recovery of nearly 8,000 metagenome-assembled genomes
576 substantially expands the tree of life. *Nat. Microbiol.* **2**, 1533–1542 (2017).

577 30. Beitel, C. W. *et al.* Strain- and plasmid-level deconvolution of a synthetic metagenome by
578 sequencing proximity ligation products. *PeerJ* **2014**, e415 (2014).

579 31. Burton, J. N., Liachko, I., Dunham, M. J. & Shendure, J. Species-level deconvolution of
580 metagenome assemblies with Hi-C-based contact probability maps. *G3 Genes, Genomes,*
581 *Genet.* **4**, 1339–1346 (2014).

582 32. Du, Y. & Sun, F. HiCBin: Binning metagenomic contigs and recovering metagenome-
583 assembled genomes using Hi-C contact maps. *bioRxiv* 2021.03.22.436521 (2021).
584 doi:10.1101/2021.03.22.436521

585 33. Baudry, L., Foutel-Rodier, T., Thierry, A., Koszul, R. & Marbouth, M. MetaTor: A

586 computational pipeline to recover high-quality metagenomic bins from mammalian gut
587 proximity-ligation (Meta3C) libraries. *Front. Genet.* **10**, 753 (2019).

588 34. Press, M. *et al.* Hi-C deconvolution of a human gut microbiome yields high-quality draft
589 genomes and reveals plasmid-genome interactions. *bioRxiv* 198713 (2017).
590 doi:10.1101/198713

591 35. Demaere, M. Z. & Darling, A. E. Bin3C: Exploiting Hi-C sequencing data to accurately
592 resolve metagenome-assembled genomes. *Genome Biol.* **20**, (2019).

593 36. Mallick, H. *et al.* Multivariable association discovery in population-scale meta-omics
594 studies. *bioRxiv* 2021.01.20.427420 (2021). doi:10.1101/2021.01.20.427420

595 37. Medema, M. H. *et al.* AntiSMASH: Rapid identification, annotation and analysis of
596 secondary metabolite biosynthesis gene clusters in bacterial and fungal genome
597 sequences. *Nucleic Acids Res.* **39**, W339 (2011).

598 38. Hannigan, G. D. *et al.* A deep learning genome-mining strategy for biosynthetic gene
599 cluster prediction. *Nucleic Acids Res.* **47**, e110 (2019).

600 39. Navarro-Muñoz, J. C. *et al.* A computational framework to explore large-scale
601 biosynthetic diversity. *Nat. Chem. Biol.* **16**, 60–68 (2020).

602 40. Brouns, F. Saccharide characteristics and their potential health effects in perspective.
603 *Frontiers in Nutrition* **7**, 75 (2020).

604 41. Lopez-Siles, M., Duncan, S. H., Garcia-Gil, L. J. & Martinez-Medina, M. *Faecalibacterium*
605 *prausnitzii*: From microbiology to diagnostics and prognostics. *ISME Journal* **11**, 841–852
606 (2017).

607 42. Yao, Q. *et al.* Potential of fecal microbiota for detection and postoperative surveillance of
608 colorectal cancer. *BMC Microbiol.* **21**, (2021).

609 43. Clemente, J. C. *et al.* The microbiome of uncontacted Amerindians. *Sci. Adv.* **1**, (2015).

610 44. Schnorr, S. L. *et al.* Gut microbiome of the Hadza hunter-gatherers. *Nat. Commun.* **5**,
611 (2014).

612 45. Dehingia, M. *et al.* Gut bacterial diversity of the tribes of India and comparison with the
613 worldwide data. *Sci. Rep.* **5**, 18563 (2015).

614 46. Bickhart, M. *et al.* Generation of lineage-resolved complete metagenome-assembled
615 genomes by precision phasing. *bioRxiv* 2021.05.04.442591 (2021).
616 doi:10.1101/2021.05.04.442591

617 47. Sereika, M. *et al.* Oxford Nanopore R10.4 long-read sequencing enables near-perfect
618 bacterial genomes from pure cultures and metagenomes without short-read or reference
619 polishing. *bioRxiv* 2021.10.27.466057 (2021). doi:10.1101/2021.10.27.466057

620 48. Sanna, S. *et al.* Causal relationships among the gut microbiome, short-chain fatty acids
621 and metabolic diseases. *Nature Genetics* **51**, 600–605 (2019).

622 49. Lloyd-Price, J. *et al.* Multi-omics of the gut microbial ecosystem in inflammatory bowel
623 diseases. *Nature* **569**, 655–662 (2019).

624 50. Milshteyn, A., Colosimo, D. A. & Brady, S. F. Accessing Bioactive Natural Products from
625 the Human Microbiome. *Cell Host and Microbe* **23**, 725–736 (2018).

626 51. Wilson, M. R., Zha, L. & Balskus, E. P. Natural product discovery from the human
627 microbiome. *Journal of Biological Chemistry* **292**, 8546–8552 (2017).

628 52. Ostaff, M. J., Stange, E. F. & Wehkamp, J. Antimicrobial peptides and gut microbiota in
629 homeostasis and pathology. *EMBO Mol. Med.* **5**, 1465–1483 (2013).

630 53. De Coster, W., D'Hert, S., Schultz, D. T., Cruts, M. & Van Broeckhoven, C. NanoPack:
631 visualizing and processing long-read sequencing data. *Bioinformatics* 237180 (2018).
632 doi:10.1093/bioinformatics/bty149

633 54. Wood, D. E., Lu, J. & Langmead, B. Improved metagenomic analysis with Kraken 2.
634 *Genome Biol.* **20**, 1–13 (2019).

635 55. Lu, J., Breitwieser, F. P., Thielen, P. & Salzberg, S. L. Bracken: estimating species
636 abundance in metagenomics data. *PeerJ Comput. Sci.* **3**, e104 (2017).

637 56. Parks, D. H., Imelfort, M., Skennerton, C. T., Hugenholtz, P. & Tyson, G. W. CheckM:
638 Assessing the quality of microbial genomes recovered from isolates, single cells, and
639 metagenomes. *Genome Res.* **25**, 1043–1055 (2015).

640 57. Lowe, T. M. & Chan, P. P. tRNAscan-SE On-line: integrating search and context for
641 analysis of transfer RNA genes. *Nucleic Acids Res.* **44**, W54–7 (2016).

642 58. Orakov, A. *et al.* GUNC: detection of chimerism and contamination in prokaryotic
643 genomes. *Genome Biol.* **22**, (2021).

644 59. Hyatt, D. *et al.* Prodigal: Prokaryotic gene recognition and translation initiation site
645 identification. *BMC Bioinformatics* **11**, 1–11 (2010).

646 60. Chaumeil, P. A., Mussig, A. J., Hugenholtz, P. & Parks, D. H. GTDB-Tk: A toolkit to classify
647 genomes with the genome taxonomy database. *Bioinformatics* **36**, 1925–1927 (2020).

648 61. Ondov, B. D. *et al.* Mash: Fast genome and metagenome distance estimation using
649 MinHash. *Genome Biol.* **17**, 132 (2016).

650 62. Cock, P. J. A. *et al.* Biopython: freely available Python tools for computational molecular
651 biology and bioinformatics. *Bioinformatics* **25**, 1422–1423 (2009).

652 63. Jain, C., Rodriguez-R, L. M., Phillippy, A. M., Konstantinidis, K. T. & Aluru, S. High
653 throughput ANI analysis of 90K prokaryotic genomes reveals clear species boundaries.
654 *Nat. Commun.* **9**, 5114 (2018).

655 64. Pasolli, E. *et al.* Extensive unexplored human microbiome diversity revealed by over
656 150,000 genomes from metagenomes spanning age, geography, and lifestyle. *Cell* **176**,
657 649–662.e20 (2019).

658 65. Wood, D. E. & Salzberg, S. L. Kraken: Ultrafast metagenomic sequence classification using
659 exact alignments. *Genome Biol.* **15**, R46 (2014).

660 66. Hsieh, T. C., Ma, K. H. & Chao, A. iNEXT: an R package for rarefaction and extrapolation of
661 species diversity (Hill numbers). *Methods Ecol. Evol.* **7**, 1451–1456 (2016).

662 67. Blin, K. *et al.* AntiSMASH 5.0: Updates to the secondary metabolite genome mining
663 pipeline. *Nucleic Acids Res.* **47**, W81–W87 (2019).

664 68. Cimermancic, P. *et al.* Insights into secondary metabolism from a global analysis of
665 prokaryotic biosynthetic gene clusters. *Cell* **158**, 412–421 (2014).

666 69. Gilchrist, C. L. M. & Chooi, Y.-H. clinker & clustermap.js: automatic generation of gene
667 cluster comparison figures. *Bioinformatics* **37**, 2473–2475 (2021).

668 70. Kautsar, S. A. *et al.* MIBiG 2.0: A repository for biosynthetic gene clusters of known
669 function. *Nucleic Acids Res.* **48**, D454–D458 (2020).

670 71. Medema, M. H., Takano, E. & Breitling, R. Detecting Sequence Homology at the Gene
671 Cluster Level with MultiGeneBlast. *Mol. Biol. Evol.* **30**, 1218 (2013).

672 72. Gallagher, K. A. & Jensen, P. R. Genomic insights into the evolution of hybrid isoprenoid
673 biosynthetic gene clusters in the MAR4 marine streptomycete clade. *BMC Genomics* **16**,
674 1–13 (2015).

675 73. Veltri, D., Kamath, U. & Shehu, A. Deep learning improves antimicrobial peptide
676 recognition. *Bioinformatics* **34**, 2740–2747 (2018).

677 74. Burdukiewicz Michał and Sidorczuk, K. *et al.* Proteomic screening for prediction and
678 design of antimicrobial peptides with ampgram. *Int. J. Mol. Sci.* **21**, 1–13 (2020).

679 75. Pinacho-Castellanos, S. A., García-Jacas, C. R., Gilson, M. K. & Brizuela, C. A. Alignment-
680 free antimicrobial peptide predictors: Improving performance by a thorough analysis of
681 the largest available data set. *J. Chem. Inf. Model.* **61**, 3141–3157 (2021).

682 76. Shen, W., Le, S., Li, Y. & Hu, F. SeqKit: A cross-platform and ultrafast toolkit for FASTA/Q
683 file manipulation. *PLoS One* **11**, (2016).

684 77. Watts, S. C., Ritchie, S. C., Inouye, M. & Holt, K. E. FastSpar: Rapid and scalable
685 correlation estimation for compositional data. *Bioinformatics* **35**, 1064–1066 (2019).

686

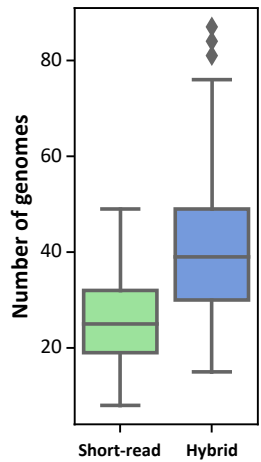
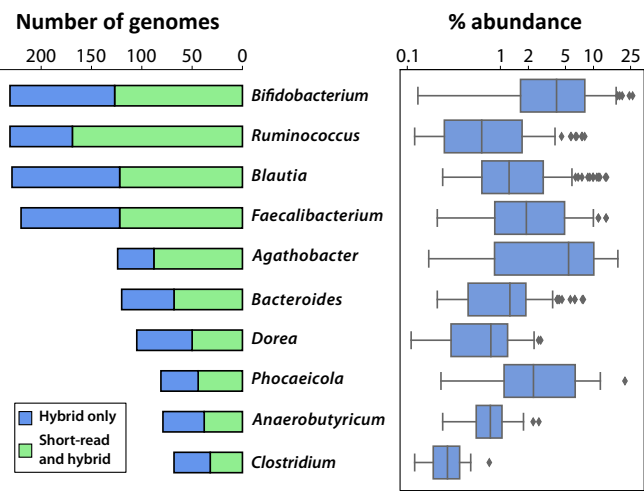
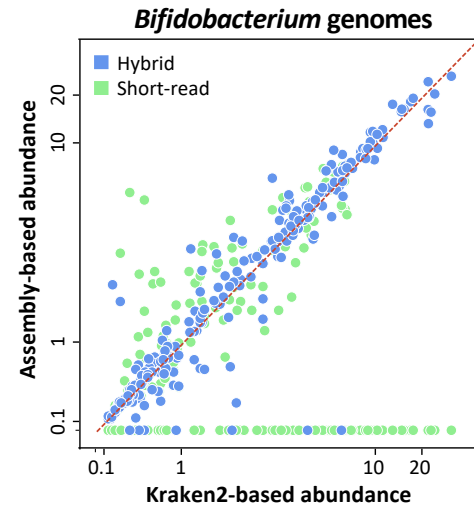
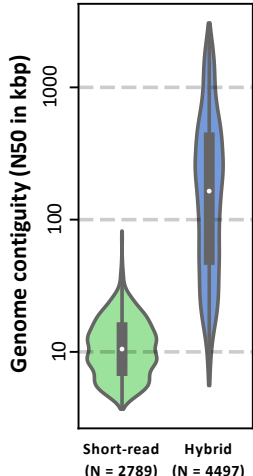
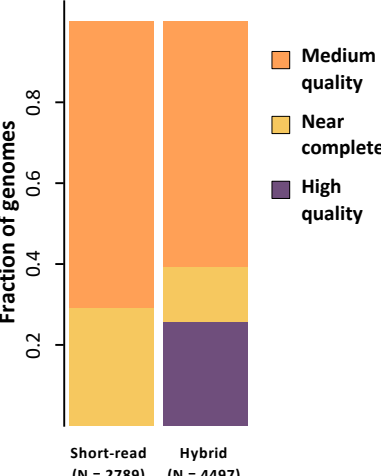
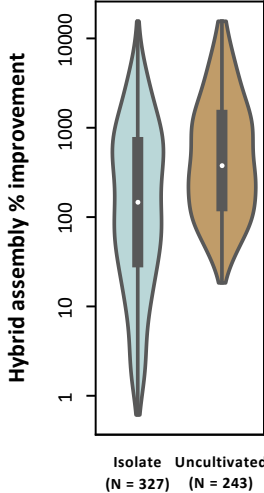
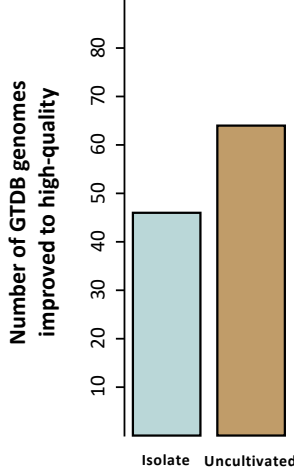
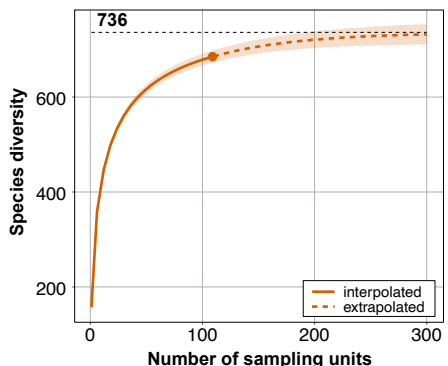
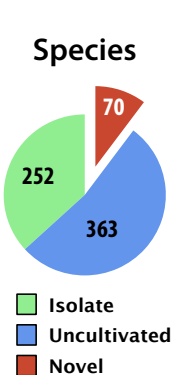
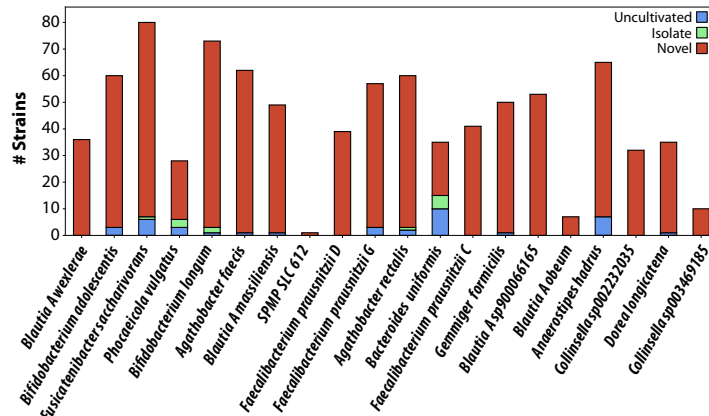
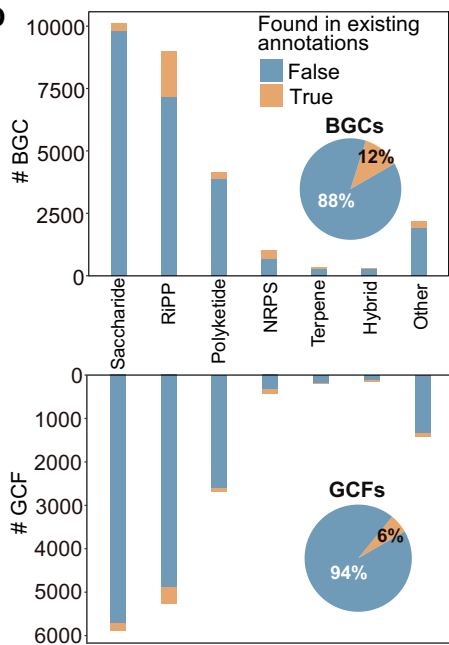
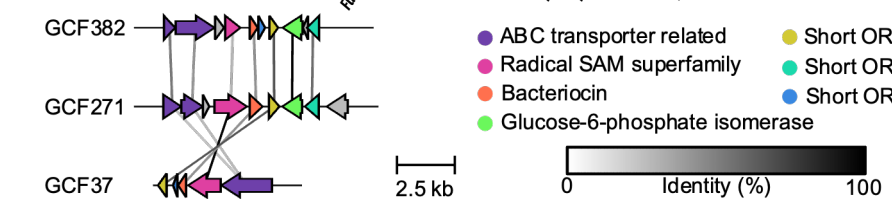
Figure 1**A****B****C****D****E****F****G**

Figure 2**A****B****C****D****E****F**